

Received: 30 September 2017

Revised: 14 November 2017


Accepted: 28 November 2017

DOI: 10.1002/gj.3129

WILEY

SPECIAL ISSUE ARTICLE

Radiometric dating of late Quaternary loess in the northern piedmont of South Tianshan Mountains: Implications for reliable dating

Yougui Song^{1,3}  | Dan Luo¹ | Jinhua Du² | Shugang Kang¹ | Peng Cheng¹ |
Chaofeng Fu²  | Xiaohua Guo³

¹State Key Laboratory of Loess and Quaternary Geology, Institute of Earth and Environment, Chinese Academy of Sciences, Xi'an, Shaanxi, China

²Key Laboratory of Western Mineral Resources and Geological Engineering, Ministry of Education of China, School of Geoscience and Land Resources, Chang'an University, Xi'an, Shaanxi, China

³Geoluminescence Dating Research Laboratory, Department of Geosciences, Baylor University, Waco, Texas, USA

Correspondence

Dr. Yougui Song, Institute of Earth Environment, Chinese Academy of Sciences, No 97 Yanxiang Road, Yanta District, Xi'an, Shaanxi, 710061, China.
Email: syg@ieecas.cn; ygsong@loess.llqg.ac.cn

Funding information

National Key Research and Development Program of China, Grant/Award Number: 2016YFA0601902; National Natural Science Foundation of China, Grant/Award Number: 41572162 and 41290253; International Partnership Program of the Chinese Academy of Sciences, Grant/Award Number: 132B61KYS20160002

Handling Editor: I. D. Somerville

Reliable chronologies are prerequisites when interpreting proxy records in terrestrial archives of Quaternary climate and environmental change. Optically stimulated luminescence (OSL) dating and accelerator mass spectrometry radiocarbon dating (AMS ¹⁴C) are commonly used to date late Quaternary loess deposits in the Chinese Loess Plateau, but the range and reliability of the two methods in Central Asia are still debated. In this study, we investigate both fine-grained quartz OSL and AMS ¹⁴C dating of a late Quaternary loess section located at the northern piedmont of the South Tianshan Mountains in Central Asia and discuss the reliability of the two radiometric dating methods. The results show that the OSL and AMS ¹⁴C ages are generally consistent with the stratigraphic sequence when the ages are younger than 25 cal ka BP, which means that both can be used to establish a reliable chronology in the Ili Basin. But beyond this age, the OSL dating method seems to be a more reliable approach. The results also supported previous dates based on medium-grained quartz OSL dating of the Ili loess in the southern piedmont of the North Tianshan Mountains. Radiocarbon ages older than 25 cal ka BP should be treated with caution, and attention must be paid to the influence of pedoturbation on OSL signals in the Central Asian loess. Multiple dating approaches for mutual authentication and exploring new dating materials are suggested in further loess chronological research. These findings will be helpful in establishing a reliable timescale and in reconstructing high-resolution environmental change in Central Asia.

KEYWORDS

AMS ¹⁴C, Ili Basin, late Quaternary, loess, OSL, reliability of ages, Tianshan Mountains

1 | INTRODUCTION

Loess is one of the best archives of past global climate change and plays an important role in understanding Quaternary climate and environmental change in arid and semi-arid areas (Liu, 1985). Central Asia is also one of the world's major loess distribution areas, with loess deposits intermittently covering the foothills and river terraces of the Tianshan Mountains, Kunlun Mountains, and Altai Mountains

(Dodonov, 1991; Dodonov & Baiguzina, 1995; Li, Song, Yan, Chen, & An, 2015). The Ili Basin is located between the South Tianshan and North Tianshan Mountains, and contains loess deposits reaching 200 m thickness (Song et al., 2014), but most of the loess natural outcrops have developed since the last glacial period. In the past two decades, many researches have focused on the loess distribution in the Ili Basin (Li et al., 2015; Shi, 2005; Song et al., 2014; Ye, 2001) and the paleoclimatic significance of various proxies such as particle size (Li, Song, Lai, Han, & An, 2016; Song, Li, et al., 2017; Ye, Dong, Yuan, & Ma, 2000), magnetism (Chen et al., 2012; Jia, Xia, Wang, Wei, & Liu, 2012; Shi, Dong, & Fang, 2007; Song, 2012; Song, Nie,

[Correction added on 12 February 2018, after first online publication: The sixth author's name has been corrected.]

et al., 2010; Song, Shi, et al., 2010), elemental geochemistry (Chen et al., 2017; Zhang et al., 2013), and minerals (Li et al., 2017; Song, Zeng, et al., 2017), yet late Quaternary loess sediments in this basin remain poorly dated. This prevents us from addressing issues such as synchronicity of abrupt climatic/environmental events on millennial timescales since the last glaciation.

Recent advances in radioactive dating have enabled independent investigation into loess age. Optically stimulated luminescence (OSL) and Accelerator Mass Spectrometry (AMS) radiocarbon (^{14}C) dating methods as the two most common radiometric techniques have been widely applied to date the Late Quaternary aeolian loess on the Chinese Loess Plateau and Northern American loess, albeit with some disagreement between the two methods (Pigati, Mcghehin, Muhs, & Bettis, 2013; Wang et al., 2014; Zech et al., 2017). Recently, attempts have been made to apply the polymineral, quartz, and K-feldspar OSL dating methods to Central Asian loess. To date, fine-grained (4–11 μm) (Feng et al., 2011; Fitzsimmons et al., 2017; Kang et al., 2015; Song, Li, Zhao, Chen, & Zeng, 2012; Youn, Seong, Choi, Abdrakhmatov, & Ormukov, 2014), medium-grained (38–63 μm) (E et al., 2012; Li et al., 2016; Song, Li, et al., 2017; Song, Lai, Li, Chen, & Wang, 2015), and coarse-grained (>63 μm) particles (Fu, Li, & Li, 2015; Li et al., 2015; Yang et al., 2014; Youn et al., 2014) have been adopted for OSL dating of the Ili and Tianshan loess; however, due to the inherent limitations of luminescence techniques and a large discrepancy between the AMS ^{14}C age and OSL age in the Ili loess (E et al., 2012; Feng et al., 2011; Kang et al., 2015; Song et al., 2015), the reliability of luminescence chronologies of loess in this area was questioned (Feng et al., 2011; Li et al., 2015; Qin & Zhou, 2017; Yang et al., 2014). Therefore, the feasibility and weakness of the two dating methods in arid Central Asia are worthy of further investigation. In this paper, fine-grained quartz OSL and AMS ^{14}C dating were used to establish stratochronological sequence of a loess section in the northern piedmont of South Tianshan Mountains, Central Asia. The reliability and limitations of these two approaches were also discussed.

2 | GEOLOGICAL BACKGROUND AND SAMPLING

The Tianshan Mountains, also called Tienshan, are a large system of mountain range situated in the Eurasia hinterland. It stretches through four countries (China, Kazakhstan, Kyrgyzstan, and Uzbekistan) with a length of 2,500 km east to west. This mountain system composes part of the basin-and-range topography. The Ili Basin is a mountainous superimposed basin that developed on the microblock sandwiched by the Tianshan Mountains (Figure 1). The trumpet-shaped basin opens to the west, and extends westward to the Gobi-desert area of Kazakhstan, receiving water vapour brought by westerlies. Because of characteristic geomorphic features, the Ili Basin has a semiarid-arid, continental climate and is dominated by high-altitude westerlies. The average annual rainfall is about 350 mm, and the mean annual temperature varies from 2.6 to 10.4 $^{\circ}\text{C}$. Peak precipitation is asynchronous with peak temperature: spring and winter are wet, whereas summer is dry. The vegetation and zonal soil transition from desert steppe, steppe to grassland, and sierozem, chestnut soil to chernozem.

Loess in the Ili Basin is mainly distributed across the piedmont of the Tianshan mountains and river terraces. The thickness of the loess varies from several meters to over 200 m (Song et al., 2014). The Zhaosu Boma (ZSB) section (42 $^{\circ}$ 41'36.08"N, 80 $^{\circ}$ 15'8.22"E) is located in the second terrace of Tekes River (upper reaches of the Ili river), near west to Boma town, 90 km southwest of Zhaosu County. It is situated in the steppe zone at the northern piedmont of the South Tianshan Mountains. In 2006, a 6.9-m-thick loess section was excavated, and geochronological and proxies (Li, Song, Qian, & Wang, 2011; Song et al., 2012; Song, Zeng, et al., 2017) indicated that it recorded the climate change history since the last glacial period. In order to further improve the comparability of the event ages and to check the reliability of the new fine-grained quartz OSL age and AMS ^{14}C data, we excavated a new section near the previous one destroyed by collapse, and collected closely-spaced dating and

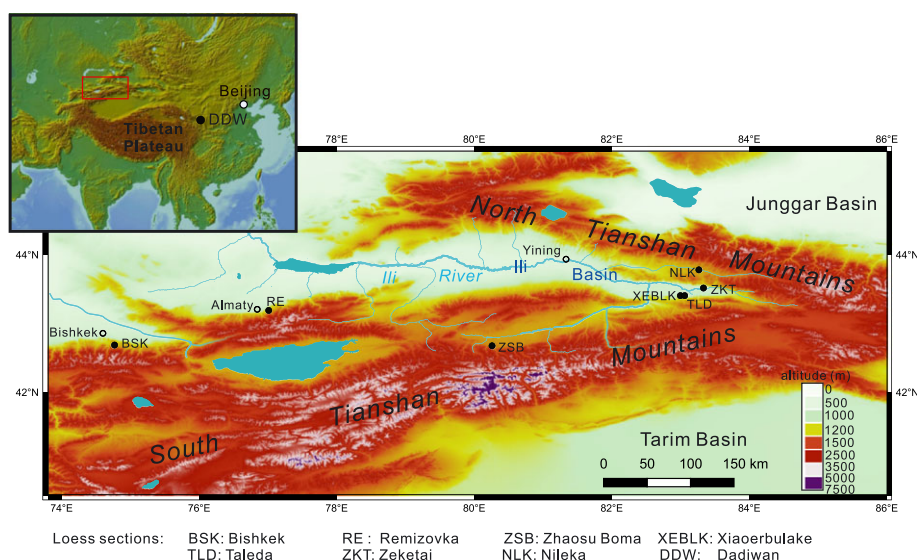


FIGURE 1 Locations of loess sections of this study and previous studies in the Ili Basin and Tianshan Mountains. Inset map shows location of the study area in Asia and Didiwan (DDW) loess section of the Chinese Loess Plateau

discrete samples. The section can be divided into four stratigraphic units. Unit 1 (the upper 0.9 m) is composed of a black, humus, and carbonate-enriched accretionary Holocene soil (Chernozem); The 0.9–6.6 m depth is a structureless yellowish silty loess (Unit 2 and Unit 4) with weakly developed light brownish palaeosol intercalated at depths of 1.9 to 4.9 m (Unit 3). Underlying the loess sequence are fluvial gravel sediments. Fourteen OSL samples were collected at 0.5 m intervals and 10 AMS ^{14}C samples were collected at 0.2–1.15 m intervals. OSL samples were collected by hammering 20 cm long stainless steel cylinders with a diameter of 5 cm into freshly cleaned profiles. The tubes were then covered with aluminium foil and sealed with opaque tape.

3 | EXPERIMENTAL METHODS

3.1 | OSL dating

3.1.1 | Sample pretreatment

All OSL samples were processed under subdued red-light conditions in the laboratory. About 3 cm of sediment at both ends of the tubes, which may have been exposed to daylight during sampling, were removed and kept for radioisotope concentration analysis. The remaining unexposed loess samples were prepared for quartz OSL equivalent dose (De) determination. The fine-grained (4–11 μm) quartz was extracted using established laboratory pretreatment procedures for Chinese loess (Forman, 1991; Lu, Wang, & Wintle, 2007). First, the remaining unexposed sediments were pretreated with 30% HCl and 30% H_2O_2 to remove carbonates and organic materials, respectively. Second, when the reactions were complete, distilled water was used to rinse the remains until the solution reached a neutral pH. Third, the fine silt (4–11 μm) fraction was extracted using sedimentation procedures based on Stokes' Law settling. Fourth, the extractions were immersed in 30% hydrofluorosilicic acid (H_2SiF_6) for 3–5 days in an ultrasonic bath to remove feldspars and obtain the fine quartz grains. Finally, the purified quartz was deposited on 9.7 mm diameter stainless steel discs for further experiments. Feldspar is sensitive to infrared while quartz is not, so the purity of the isolated quartz grains was checked by the regenerative dose infrared stimulated luminescence (IRSL) signal (Duller, 2003). If the IRSL signal in the sample was almost negligible or close to the background, the chemically isolated quartz was sufficiently pure for OSL dating.

3.1.2 | Determination of the equivalent dose

The single-aliquot regenerative-dose (Murray & Wintle, 2000) protocol was used in this study. All OSL samples were analysed in the Institute of Earth Environment, Chinese Academy of Sciences, using an automated luminescence measurement system (Daybreak 2200) equipped with infrared (880 ± 60 nm) and blue (470 ± 5 nm) LED units and a $^{90}\text{Sr}/^{90}\text{Y}$ beta source for irradiation. The OSL signals were measured for 100 s at a readout temperature of 130 $^\circ\text{C}$, together with the natural aliquots, they were preheated to 260 $^\circ\text{C}$ for 10 s for the removal of unstable signals. Signals were detected through an EMI 9235QA photomultiplier tube coupled with 7.5 mm U-340 glass filter. The dose of the artificial light was $^{90}\text{Sr}/^{90}\text{Y}$, and the dose rate was

0.038 Gy/s (4–11 μm). For the equivalent dose (De) determination, the net luminescence signal was calculated using the first 5 s integral of the decay curve subtracted by that of the last 5 s. A saturating exponential function was used to calculate the dose response curves, that is, the OSL growth curve, to determine the equivalent dose of the sample.

3.1.3 | Determination of environmental dose rate

The environmental dose rate is one of the important parameters of OSL. The ambient radiation dose absorbed by the sample is the effect of α , β , γ rays of radionuclides (^{235}U , ^{238}U , ^{232}Th , and ^{40}K) in their own and surrounding sediments, as well as their decay product, and partly from cosmic rays. The concentrations of uranium (U) and thorium (Th) were measured using inductively coupled plasma mass spectrometry, and inductively coupled plasma emission spectrometry was used to determine the potassium (K) concentration. Given that the loess samples are from the Ili Basin, which is in a semi-arid to semi-humid, and based on measured water content variations and knowledge of paleoclimatic change in Central Asia, the mean water contents of the loess during geological time were assumed to be $15 \pm 5\%$. The environmental dose rate was calculated based on the concentrations of radioactive elements such as U, Th, and K, and background parameters including latitude, longitude, elevation, burial depth, and sediment density of samples (Adamiec & Aitken, 1998; Prescott & Hutton, 1994).

3.2 | AMS ^{14}C dating

All radiocarbon analyses were conducted at the centre of Xi'an AMS in the Institute of Earth Environment, Chinese Academy of Sciences. The dating material was humin component from the remaining alkali-insoluble fraction. The pre-treatment procedure followed a conventional acid–base–acid method (Cheng, Zhou, Wang, Lu, & Du, 2013; Cheng, Zhou, Yu, & Zeng, 2007; Zhou et al., 2016). All samples were dried thoroughly at room temperature and subsequently sieved to remove visible plant remains, such as rootlets. The bulk samples were treated with 1 N HCl at 70 $^\circ\text{C}$ for 2 hr to remove possible inorganic carbonate. The samples were then thoroughly rinsed with distilled water until neutral, followed by 1 N NaOH in a water bath for another 2 hr to ensure the complete removal of humic and fulvic acids. The samples were rinsed repeatedly with deionized water until neutral and 1 N HCl was again added to the samples to ensure that the samples would be pH neutral. Then, the residues were dried at 60 $^\circ\text{C}$ in an oven. In order to convert the isolated humin acid into a graphite sample, we placed the extractions and CuO powder into a vacuum system to combust with an improved pyrolysis method (Cheng et al., 2013) that produces CO_2 gas. The purified CO_2 gas was then fed into a synthetic device, where the CO_2 was converted catalytically to graphite using a zinc reduction method (Jull, 2007). The zinc particles were used as the reducing agent and iron powder as a catalyst to synthesize graphite. Finally, the graphite was pressed into target material for AMS measurement (Cheng et al., 2007). The ^{14}C content of the graphite was measured in the Xi'an AMS facility with a measurement uncertainty of $^{14}\text{C}/^{12}\text{C}$ for better than 0.2% in routine operation for a modern sample. The

minimum measurable ratio of $^{14}\text{C}/^{12}\text{C}$ in this machine is 3.1×10^{-16} (Cheng et al., 2013).

4 | RESULTS

4.1 | Luminescence characteristics and OSL ages

Figure 2 illustrates the fine-grained quartz OSL D_e analysis of two samples (ZSB200 and ZSB500) using the single aliquot regenerative dose protocol (Murray & Wintle, 2003). From the OSL decay curves of ZSB loess samples (Figure 2a,c), the natural signals decay faster, the signals of both natural and test samples can be reduced by about 90% in the first 5 s of stimulation, indicating that the OSL signal is dominated by the fast component. The growth curves (Figure 2b,d) were well represented using the exponential plus linear fitting. According to the growth curves, we obtained the equivalent dose of these samples, equivalent doses of ZSB200 and ZSB500 sample are 78.86 Gy and 121 Gy, respectively. The luminescence decay curves of the other samples are like these of the two samples, and their luminescent properties are not significantly different.

The radionuclide concentrations, dose rate, D_e values, and OSL dating results are shown in Table 1. U, Th, and K contents range from 2.28 to 4.34, 10.79 to 12.90 mg/kg and from 2.03% to 2.44%, respectively, resulting in dose rates between 4.09 and 4.64 Gy/ka.

The dose rates are generally close to those of fine-grained quartz from piedmont Bishkek (BSK) loess in the Kyrgyz Tian Shan (Figure 1; Youn et al., 2014), but larger than those of medium-grained quartz from the Zeketai (ZKT) loess section (Figure 1) in the eastern Ili Basin (E et al., 2012) and those of fine-grained quartz from the Chinese Loess Plateau (Lu et al., 2007). The OSL ages are ranged from 1.05 to 43.77 ka. In general, the OSL age is consistent with the stratigraphic sequence (Figure 3). However, there are several inconsistent samples (Table 1 and Figure 3). The OSL ages from 0.5 to 2.5 m in depth are concentrated at 18 ka BP. Especially, the OSL age at 1 m depth (ZSB100: 21.13 ± 1.20 ka) is aberrant and older than those of the upper or lower samples. In addition, two samples around 6.0 and 6.4 m in depth appear inconsistent, but are still consistent within errors range.

4.2 | AMS ^{14}C ages

The AMS ^{14}C dating results are shown in Table 2 and Figure 3. The conventional ages were calibrated using CalIB7.02 software based on the IntCal13 calibration curve (Reimer, Reimer, & Blaauw, 2013). From the age-depth plot (Figure 3a), it can be observed that the uppermost 7 AMS ^{14}C ages ranging from 0.88 to 28 cal ka BP are generally consistent with the stratigraphic succession, except for the ZSB300 sample, the other dates deeper than 4 m, however, do not increase with depth, and their ages are concentrated at around 28 cal ka BP.

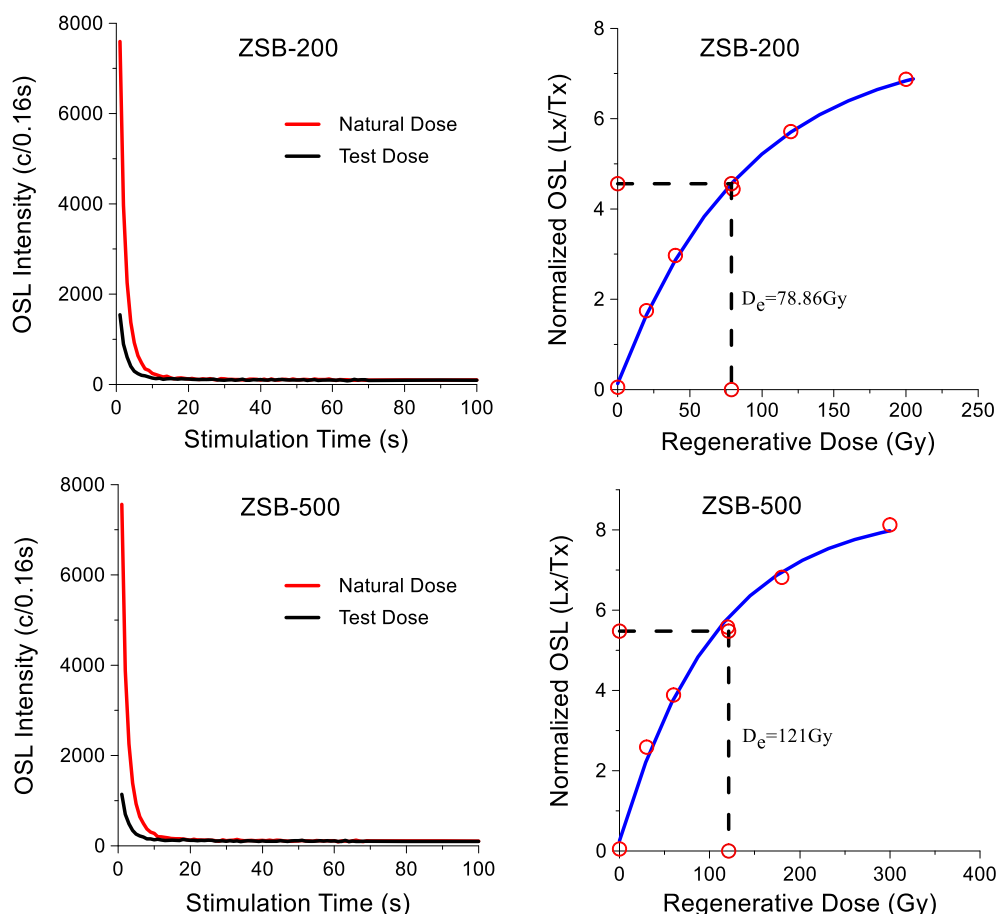


FIGURE 2 Optically stimulated luminescence (OSL) decay and growth curves by single-aliquot regenerative-dose protocol of typical loess samples

TABLE 1 Optically stimulated luminescence (OSL) dating results of the samples from the ZSB loess section

Sample no.	Depth (m)	U (ppm)	Th (ppm)	K (%)	Water content (%)	Dose rate (Gy/ka)	De value (Gy)	OSL age (ka)
ZSB0	0.0	2.28	11.55	2.19	15 ± 5	4.15 ± 0.16	4.36 ± 0.40	1.05 ± 0.10
ZSB50	0.5	2.63	12.02	2.09	15 ± 5	4.09 ± 0.16	69.72 ± 2.94	17.05 ± 0.98
ZSB100	1.0	3.04	11.42	2.13	15 ± 5	4.16 ± 0.16	87.88 ± 3.64	21.13 ± 1.20
ZSB150	1.5	3.62	10.46	2.03	15 ± 5	4.14 ± 0.17	70.42 ± 3.38	17.00 ± 1.06
ZSB200	2.0	4.34	10.85	2.14	15 ± 5	4.49 ± 0.18	78.86 ± 3.71	17.56 ± 1.09
ZSB250	2.5	3.54	11.16	2.25	15 ± 5	4.35 ± 0.17	78.42 ± 4.79	18.05 ± 1.32
ZSB300	3.0	3.21	11.12	2.23	15 ± 5	4.21 ± 0.17	106.73 ± 6.75	25.35 ± 1.90
ZSB350	3.5	3.33	12.01	2.31	15 ± 5	4.39 ± 0.18	121.04 ± 7.22	27.55 ± 1.98
ZSB400	4.0	3.50	12.90	2.44	15 ± 5	4.64 ± 0.19	131.54 ± 7.02	28.36 ± 1.89
ZSB450	4.5	3.13	11.55	2.16	15 ± 5	4.14 ± 0.17	142.49 ± 11.52	34.43 ± 3.10
ZSB500	5.0	3.44	11.17	2.06	15 ± 5	4.10 ± 0.17	147.32 ± 7.00	35.92 ± 2.24
ZSB550	5.5	3.12	10.79	2.26	15 ± 5	4.15 ± 0.17	181.83 ± 9.69	43.77 ± 2.92
ZSB600	6.0	3.58	11.78	2.27	15 ± 5	4.38 ± 0.18	191.25 ± 14.67	43.63 ± 3.78
ZSB640	6.4	3.58	12.21	2.31	15 ± 5	4.45 ± 0.18	187.57 ± 11.17	42.14 ± 3.03

This likely indicates an underestimation of radiocarbon dates for the strata at depths of 3.95–6.6 m.

5 | DISCUSSION

5.1 | Comparison of OSL ages and AMS ¹⁴C ages

In general, OSL ages are consistent with corresponding AMS ¹⁴C ages and the stratigraphic sequence in the upper 4 m interval (Figure 3a). The consistent AMS ¹⁴C and OSL ages suggest that these ages are reliable and should reflect the real age of sedimentation. However, we note the conspicuous age discrepancies between AMS ¹⁴C ages and OSL ages within the upper 1.2 m. In fact, the bottom of the Holocene soil observed in the field investigation is located at a depth of 0.9 m. We collected an AMS ¹⁴C sample (ZSB85) around the boundary, and its calibrated radiocarbon age is 4013–4229 cal BP, which is younger than we estimated. It may be caused by carbonate leaching during the modern precipitations. The overestimation of OSL age at ZSB100 may be caused by disturbance infiltration of fines or pedogenesis (Yang et al., 2014). Bioturbation associated with a paleo-surface often mixes full or partial solar resets grains with older grains at depth from the C horizon. The concentrated OSL ages from 0.5 to 2.5 m in depth could imply rapid deposition during the last glacial maximum observed in Remizovka (RE) loess section near Almaty in the northern piedmont of South Tianshan Mountains (Fitzsimmons et al., 2017) and in Xiaerbulake (XEBLK) loess section in the eastern Ili Basin (Li et al., 2016; Figure 1). Deeper than 4 m, the OSL ages are significantly older than the corresponding AMS ¹⁴C ages. The AMS ¹⁴C ages are mainly concentrated at 27–28 cal ka BP. The differences between the OSL and AMS ¹⁴C ages increase with depth, and reach a maximum of 15.85 ka. The anomalous OSL ages at the bottom may be affected by the fluvial process during the deposit process. According to the linear extrapolation of OSL dates, the bottom of this section is about 50 ka BP, which is younger than that of the previous ZSP section (Song et al., 2012).

The AMS ¹⁴C ages are much younger than fine-grained quartz OSL ages, similar to observations of the other loess sequences in Central Asia (E et al., 2012; Kang et al., 2015; Song et al., 2015; Youn et al., 2014). The OSL and radiocarbon ages of Nilke (NLK) loess section in the eastern Ili Basin (Figure 1) agree well for ages younger than 30 cal ka BP; however, beyond this age, no consistent increase in AMS ¹⁴C ages with depth, while OSL ages continue to increase with depth (Song et al., 2015; Figure 3b). Discrepancy between ¹⁴C ages of snails and the fine-grained (4–11 μm) or medium-grained (38–63 μm) quartz OSL ages were also found in the Zeketai (ZKT) section (E et al., 2012; Feng et al., 2011; Figure 1). The OSL and ¹⁴C ages of carbonate and bulk organic matter of the Dadiwan (DDW) soil and loess samples in the western CLP (Figure 1) exhibited significant deviation when the calibrated ages were older than 26 (carbonate) or 34 ka (bulk organic matter; Figure 3c; Wang et al., 2014). Consistent observations were also made in other lacustrine sediments from northwestern China. The chronological results of late Quaternary lacustrine sequences in the Qaidam Basin and Tengger Desert also suggested that the radiocarbon dating technique apparently underestimates the age of the strata of >30 ka BP, and most of the published radiocarbon ages (e.g., older than ~30 ka BP) should be treated with caution: perhaps their geological implications should be reevaluated (Long & Shen, 2014).

5.2 | Implications for establishing reliable ages

Reliable chronologies are prerequisites for accurate proxy interpretations of terrestrial archives of Quaternary climate and environmental change. Radiometric techniques including radiocarbon (AMS and conventional) and luminescence (TL/OSL) have been widely used to date late Quaternary sediments. The luminescence technique directly dates the sediment (quartz and K-feldspar grains) and provides burial ages; meanwhile, the radiocarbon technique yields ages representing the time elapsed because the living system was last in equilibrium with atmospheric ¹⁴C and became closed after burial. To decide which technique yields the most accurate ages is not possible without

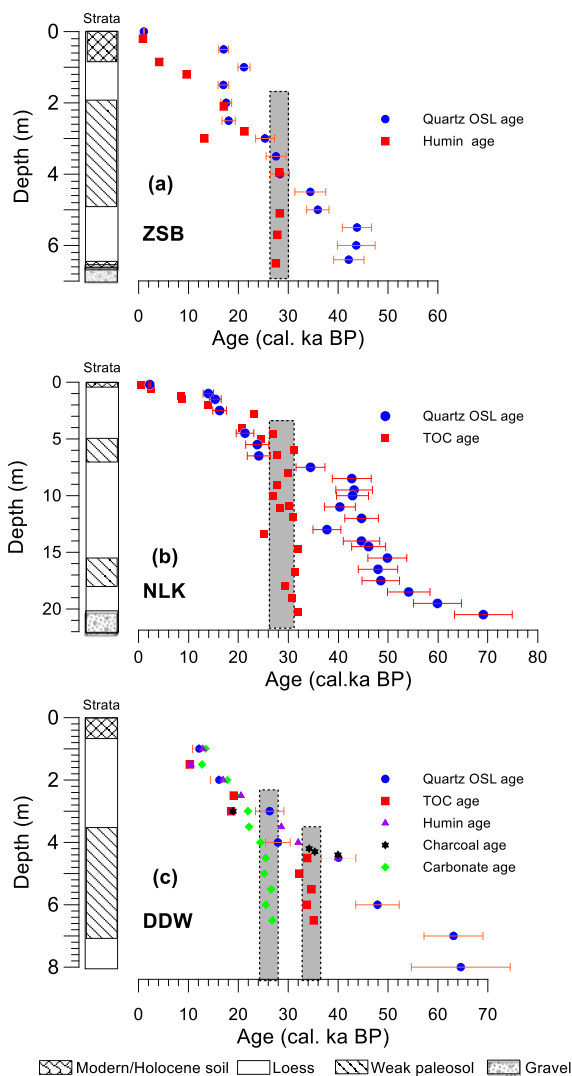


FIGURE 3 Age-depth models of optically stimulated luminescence (OSL) ages and AMS ^{14}C ages from the ZSB loess section and Nilka (NLK) loess section (Song et al., 2015) in the Ili Basin and Dadiwan (DDW) loess section (Wang et al., 2014) in the western Chinese loess plateau. TOC = total organic carbon

TABLE 2 Accelerator mass spectrometry radiocarbon dating results of the ZSB loess section

Sample no	Depth(m)	Dating materials	$\delta^{13}\text{C}$ (‰)	Date (BP)	Age Cal BP (1 σ)
ZSB20	0.2	Humin	-22.30	990 \pm 33	803-952
ZSB85	0.85	Humin	-21.30	3765 \pm 42	4,013-4,229
ZSB120	1.2	Humin	-25.00	8,710 \pm 30	9,560-9,700
ZSB210	2.1	Humin	-32.94	14,070 \pm 70	16,930-17,220
ZSB280	2.8	Humin	-19.90	17,557 \pm 82	21,062-21,360
ZSB300	3	Humin	-22.64	11,270 \pm 40	13,120-13,220
ZSB395	3.95	Humin	-23.32	23,410 \pm 80	28,050-28,380
ZSB510	5.1	Humin	-20.31	23,560 \pm 80	28,140-28,480
ZSB570	5.7	Humin	-19.46	23,712 \pm 137	27,675-27,901
ZSB650	6.5	Humin	-13.82	23,248 \pm 93	27,414-27,603

independent absolute chronological data based on another method. Loess contains abundant quartz and feldspar, making it an ideal material for testing luminescence techniques. Fine (4–11 μm), medium (38–63 μm), and coarse (63–90, 90–125 μm) quartz grains are often chosen for the dating of loess, and all have been demonstrated to provide reliable chronologies for loess on the CLP (Roberts, 2008). At present, all these different grain sizes in the quartz OSL method have been investigated in the late Quaternary loess sediments mentioned in Section 1. In contrast, the paucity of organic material in the loess sediments in this arid area makes radiocarbon dating difficult.

There is controversy regarding the reliability of the two radiometric methods. Feng et al. (2011) considered that the loess TL and OSL clocks in the ZKT section were not completely zeroed when loess was deposited primarily by deflation from local riverbeds, such that the quartz OSL ages are overestimated, and the ^{14}C ages are more reliable. Youn et al. (2014) also quantified the different luminescence characteristics of different quartz grain sizes of Bishkek loess to incomplete bleaching at deposition and post-depositional processes; these may be responsible for the overestimation of fine-grained compared to coarse-grained quartz, leading them to believe that the coarse-grained quartz OSL ages are more reliable. However, the OSL ages of coarse-grained quartz fractions of samples NRO-11 and NRO 17 are much younger than that of fine-grained quartz (Youn et al., 2014). On the other hand, E et al. (2012) argued that the quartz OSL ages provide an accurate chronology of the ZKT loess, because some taxa incorporated ^{14}C -deficient carbon and chemical alteration of shell carbonate and contamination of the organic material by humic acids during shell formation. Moreover, the medium-to-long aeolian transport distances of dust will promote the complete bleaching or removal of the quartz OSL signal prior to deposition (Roberts, 2008). Recent similar chronological works also support the reliability of quartz OSL chronologies of the Taled (TLD) loess section (Kang et al., 2015), the NLK loess section (Song et al., 2015) in the Ili Basin (Figure 1).

However, the coarse-grained quartz OSL results from the NLK loess section indicate that the overdispersion values for the equivalent dose distributions were very high (from $38 \pm 5\%$ to $66 \pm 8\%$). The high over-dispersion of the coarse quartz grains dose may increase the uncertainty of the dose determination (e.g., Yang et al., 2014; Youn et al., 2014). Yang et al. (2014) argued that extensive pedogenic mixing or considerable effects of bioturbation may be the dominant process interfering with loess deposition in the NLK section. Other loess sections, such as ZKT (E et al., 2012; Feng et al., 2011) and TLD (Shi, 2005), XEBLK (Li et al., 2016) in the Ili Basin (Figure 1) or adjacent areas such as RE loess section near Almaty (Machalett et al., 2006) also show evidence for pedoturbation, and OSL reversals were observed at the base of paleosols or altered loess. The newest comparative study of three luminescence dating procedures using two mineral fractions has been applied to date ZKT loess (Qin & Zhou, 2017). The results indicated that the OSL ages of fine-grained quartz were in stratigraphic order and range from 37 to 61 ka, but were $\sim 30\%$ younger than the post-infrared infrared stimulated luminescence (pIRIR) ages of both fine- and medium-grained polyminerals. They considered that the quartz OSL ages of loess in this region were likely to be underestimated, especially for samples older than 40 ka, and the polymineral or potassium feldspar pIRIR signal were reliable. But they did not give

further explanations about why underestimation of fine-grained quartz OSL method or why later two methods are believable. Thus, it is still a challenge to obtain reliable quartz OSL ages. A single-grain Post-IR IRSL dating method for K-feldspar (e.g., Fu et al., 2015; Nian, Bailey, & Zhou, 2012; Trauerstein, Lowick, Preusser, & Schlunegger, 2014) or the polymineral or K feldspar pIRIR might be developed in the future to date these poorly bleached samples. Further investigation of multiple dating approaches is helpful to understand the accuracy and reliability of OSL loess dating in the Ili Basin even in arid Central Asia.

Radiocarbon dating is the most commonly used method to establish chronologies of late Quaternary sediments. The datable materials in loess are usually organic macrofossils (e.g., plant remains, charcoals), gastropod shells, rhizoliths, carbonates, and soil organic matter (SOM) or total organic carbon of bulk sediments, new datable materials such as bulk *n*-alkanes (Zech et al., 2017) and earthworm calcite granules (Moine et al., 2017; Prud'homme et al., 2015). These might have great potential for Last Glacial loess dating. Charcoals are ideal datable materials and are widely accepted as materials yielding very reliable ^{14}C ages, but are difficult to find in sufficient quantities for dating in arid areas. Rhizoliths are root systems encased in mineral matter, which are affected by the growth. Small terrestrial gastropod shells (mainly Succineidae) have been used successfully to date late Quaternary loess deposits in Alaska and the Great Plains in USA (Pigati et al., 2013; Pigati, Mcgeehin, Muhs, Grimley, & Nekola, 2015). But different taxa contain different amounts of old carbon, which leads to the inaccuracy of their ages. Some of gastropod shells may incorporate ^{14}C -deficient (or dead) carbon from the local carbonate-rich substrate during shell formation (Pigati et al., 2013), thereby producing anomalously old ages (Ujvari, Molnar, Novothny, & Kovacs, 2014). Thirteen radiocarbon dates on snail shells from the upper 12 m in ZKT section concentrated mainly around 6–8 ka BP (Feng et al., 2011), which were much younger than their thermoluminescence ages (40–60 ka; Ye, 2001). The reliability of gastropod shell radiocarbon dating still requires further investigation in this Central Asia area. Carbonate and SOM/total organic carbon from paleosols formed in the loess are often underestimated (Figure 3), caused by incorporation of younger materials through bioturbation, penetration, and rootlet decomposition. The underestimation of radiocarbon ages increases uncertainty and complexity of loess geochronology and paleoenvironment reconstruction.

Despite the above limitations, radiocarbon dating of various fractions (such as SOM, humin fraction, charcoal, and carbonate) of loess–paleosol sequences in the CLP are broadly consistent and within the measurement uncertainties when sample ages are younger than 25 cal ka BP (Figure 3c), and they also agree with OSL ages (Wang et al., 2014). Therefore, in some sense, both AMS ^{14}C dates and OSL dates of loess sediments from either the CLP or the Ili Basin are found to be reliable, when their ages are younger than 25 cal ka BP (Figure 3). Unfortunately, there are no charcoal dates over 30 cal ka BP, which hampers us to verify its reliability or accuracy. Our previous study comparing OSL and AMS ^{14}C ages of the NLK loess section in the Ili Basin (Song et al., 2015) revealed that increasing trend in AMS ^{14}C ages stopped at around 30 cal ka BP, but the OSL age continued to increase (Figure 3b). This age (30 cal ka BP) seems to represent the upper limit of reliable radiocarbon dating of aeolian loess in this

section. The new results in this study further support the existence of this threshold value for radiocarbon dating in this region. Equivalent threshold values have also been found in loess or lacustrine sediments in other arid regions as mentioned above, ranging from 25 to 34 cal ka BP (Figure 4; Lai, Mischke, & Madsen, 2013; Lai, Wintle, & Thomas, 2007; Long & Shen, 2014; Wang et al., 2014). Calculated AMS ^{14}C dates older than 25 ka BP measured in some arid regions may need to be reconsidered (Lai et al., 2007). In contrast, the aeolian fine-grained nature of loess implies medium-to-long transport distances offering ample opportunities for bleaching or removing the quartz OSL signal prior to deposition (Roberts, 2008). Therefore, the radiocarbon dating method should be treated with caution when dating relatively older (>25 cal ka BP) samples from the Central Asian loess.

The main reason for the underestimation of ^{14}C ages may be attributed to carbon contamination induced by organic matter from secondary pedogenic carbonate or chemical alternation (Briant, 2012). Previous studies (Hatté, Morvan, Noury, & Paterne, 2001; Pigati, Quade, Wilson, Jull, & Lifton, 2007) showed that the impact of contamination increases with increasing age. For most organic samples, the small amount of secondary carbon (<1–2%) that is left behind by the acid–base–acid treatment can result in significant errors for old samples because the impact of contamination increases with age. For example, a 2% contamination with modern carbon of a 15 ka sample may lead to only a minor age underestimation, whereas the same contamination for a 60 ka sample would yield an age estimate of only ~30 ka (Pigati et al., 2007). Thirty-three pairs of OSL and AMS ^{14}C samples with the same depth from the ZSB and NLK sections in the Ili Basin and the DDW loess section in the western CLP were selected and projected onto the carbon contamination ^{14}C chart (Figure 4). It can be seen that the ages <25 cal ka BP, OSL, and AMS ^{14}C of various fractions have similar ages, but beyond this age,

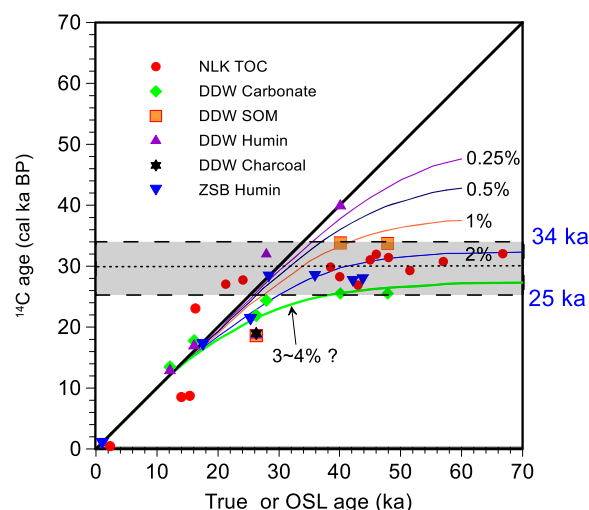


FIGURE 4 Impact of modern contamination on measured radiocarbon ages compared with true or optically stimulated luminescence (OSL) ages (modified from Pigati et al., 2007). The paired accelerator mass spectrometry radiocarbon dating and OSL ages from this study (ZSB) and Nilka (NLK) section (Song et al., 2015) and Dadiwan (DDW) section (Wang et al., 2014). TOC = total organic carbon

AMS ^{14}C dates do not increase significantly with increasing OSL age. The AMS ^{14}C ages >25 cal ka BP are scattered between 2% and 3–4% of the modern carbon contamination. Modern carbon contamination is likely to be the main cause of underestimation of radiocarbon, consistent with previous discussions (Song et al., 2015). In further radiocarbon dating of Central Asian loess, we should pay more attentions to find charcoal and explore new datable materials such as bulk *n*-alkanes (Zech et al., 2017) and earthworm calcite granules (Moine et al., 2017; Prud'homme et al., 2015).

6 | CONCLUSIONS

In this study, we applied both fine-grained quartz OSL and AMS ^{14}C dating to a late Quaternary loess section from the Ili Basin margin in the northern piedmont of South Tianshan Mountains. The results show that the OSL and AMS ^{14}C ages are generally consistent with the stratigraphic sequence when the ages are younger than 25 cal ka BP, which means that both can be used to establish a reliable chronology in the region. Beyond this age, the OSL dating method seemed to be the more reliable approach. The underestimation of radiocarbon ages could have been caused by 2–4% carbon contamination associated with organic matter from secondary pedogenic carbonate and chemical alteration. The results also supported previous medium-grained quartz OSL dating of the Ili loess in the southern piedmont of North Tianshan. Radiocarbon ages older than 25 cal ka BP should be treated with cautions, and attentions must be paid to the influence of pedoturbation on OSL signals in the Central Asian loess. Multiple dating approaches for mutual authentication and exploring new dating materials are suggested in further loess chronological research. These findings will be helpful in establishing reliable timescales and in reconstructing high-resolution environmental change in Central Asia.

ACKNOWLEDGEMENTS

This work was supported by the National Key Research and Development Program of China (2016YFA0601902), International Partnership Program of the Chinese Academy of Sciences (132B61KYS20160002), and National Natural Science Foundation of China (41572162, 41290253). We would like to thank Junchao Dong, Chuangxiang Li, Mengxiu Zeng, and Xinxin Li for their assistance during fieldwork. We thank the executive editor Prof. Ian Somerville and two anonymous reviewers for their constructive comments, which helped us to improve the manuscript. We also thank Dr. David Chandler for his critical language editing and polishing.

ORCID

Yougui Song  <http://orcid.org/0000-0003-0064-3260>

Chaofeng Fu  <http://orcid.org/0000-0002-5056-4256>

REFERENCES

- Adamiec, G., & Aitken, M. J. (1998). Dose–rate conversion factors: Update. *Ancient TL*, 16, 35–50.
- Briant, R. M. (2012). Luminescence dating indicates radiocarbon age underestimation in late Pleistocene fluvial deposits from eastern England. *Quaternary International*, 279–280(8), 67–67.
- Chen, Q., Liu, X. M., Heller, F., Hirt, A., Lü, B., Guo, X. L., ... Guo, H. (2012). Susceptibility variations of multiple origins of loess from the Ily Basin (NW China). *Chinese Science Bulletin*, 57(15), 1844–1855.
- Chen, X., Song, Y., Li, J., Fang, H., Li, Z., Liu, X., ... Orozbaev, R. (2017). Size-differentiated REE characteristics and environmental significance of aeolian sediments in the Ili Basin of Xinjiang, NW China. *Journal of Asian Earth Sciences*, 143, 30–38.
- Cheng, P., Zhou, W., Wang, H., Lu, X., & Du, H. (2013). ^{14}C dating of soil organic carbon (soc) in loess–paleosol using sequential pyrolysis and accelerator mass spectrometry (AMS). *Radiocarbon*, 55(2–3), 563–570.
- Cheng, P., Zhou, W., Yu, H., & Zeng, Y. (2007). Advances in radiocarbon dating researches in the loess–paleosol sequences. *Marine Geology and Quaternary Geology*, 27(2), 85–89 (in Chinese with English abstract).
- Dodonov, A. E. (1991). Loess of Central Asia. *GeoJournal*, 24, 185–194.
- Dodonov, A. E., & Baiguzina, L. L. (1995). Loess stratigraphy of central Asia: Paleoclimatic and palaeoenvironmental aspects. *Quaternary Science Review*, 95, 707–720.
- Duller, G. a. T. (2003). Distinguishing quartz and feldspar in single grain luminescence measurements. *Radiation Measurements*, 37(2), 161–165.
- E, C. Y., Lai, Z. P., Sun, Y. J., Hou, G. L., Yu, L. P., & Wu, C. Y. (2012). A luminescence dating study of loess deposits from the Yili River basin in western China. *Quaternary Geochronology*, 10, 50–55.
- Feng, Z. D., Ran, M., Yang, Q. L., Zhai, X. W., Wang, W., Zhang, X. S., & Huang, C. Q. (2011). Stratigraphies and chronologies of late Quaternary loess–paleosol sequences in the core area of the central Asian arid zone. *Quaternary International*, 240(1–2), 156–166.
- Fitzsimmons, K. E., Sprafke, T., Zielhofer, C., Günter, C., Deom, J.-M., Sala, R., & Iovita, R. (2017). Loess accumulation in the Tian Shan piedmont: Implications for palaeoenvironmental change in arid Central Asia. *Quaternary International*, in press, <https://doi.org/10.1016/j.quaint.2016.1007.1041>
- Forman, S. L. (1991). Late Pleistocene chronology of loess deposition near Luochuan, China. *Quaternary Research*, 36(1), 19–28.
- Fu, X., Li, S.-H., & Li, B. (2015). Optical dating of aeolian and fluvial sediments in north Tian Shan range, China: Luminescence characteristics and methodological aspects. *Quaternary Geochronology*, 30(Part B), 161–167.
- Hatté, C., Morvan, J., Noury, C., & Paterne, M. (2001). Is classical acid-alkali-acid treatment responsible for contamination? An alternative proposition. *Radiocarbon*, 43(2A), 177–182.
- Jia, J., Xia, D. S., Wang, B., Wei, H. T., & Liu, X. B. (2012). Magnetic investigation of late Quaternary loess deposition, Ili area, China. *Quaternary International*, 250, 84–92.
- Jull, A. J. T. (2007). Radiocarbon dating: AMS method. In S. A. Elias (Ed.), *Encyclopedia of Quaternary Science* (pp. 2911–2918). Oxford: Elsevier.
- Kang, S., Wang, X., Lu, Y., Liu, W., Song, Y., & Wang, N. (2015). A high-resolution quartz OSL chronology of the Taledo loess over the past ~30 ka and its implications for dust accumulation in the Ili Basin, Central Asia. *Quaternary Geochronology*, 30, 181–187.
- Lai, Z., Mischke, S., & Madsen, D. (2013). Paleoenvironmental implications of new OSL dates on the formation of the "Shell bar" in the Qaidam Basin, northeastern Qinghai-Tibetan Plateau. *Journal of Paleolimnology*, 51(2), 197–210.
- Lai, Z., Wintle, A. G., & Thomas, D. S. G. (2007). Rates of dust deposition between 50 ka and 20 ka revealed by OSL dating at Yuanbao on the Chinese Loess Plateau. *Palaeogeography, Palaeoclimatology, Palaeoecology*, 248(3–4), 431–439.
- Li, C., Song, Y., Qian, L., & Wang, L. (2011). History of climate change recorded by grain size at the Zhaosu loess section in the Central Asia since the last glacial period. *Acta Sedimentologica Sinica*, 29(6), 1170–1179 (in Chinese with English abstract).
- Li, G., Wen, L., Xia, D., Duan, Y., Rao, Z., Madsen, D. B., ... Chen, F. (2015). Quartz OSL and K-feldspar pRIR dating of a loess/paleosol sequence from arid central Asia, Tianshan Mountains, NW China. *Quaternary Geochronology*, 28(Supplement C), 40–53.

- Li, Y., Song, Y., Zeng, M., Lin, W., Orozbaev, R., Cheng, L., ... Halmurat, T. (2017). Evaluating the paleoclimatic significance of clay mineral records from a late Pleistocene loess-paleosol section of the Ili Basin, Central Asia. *Quaternary Research*, 1–14 in press. <https://doi.org/10.1017/qua.2017.58>
- Li, Y., Song, Y. G., Lai, Z. P., Han, L., & An, Z. S. (2016). Rapid and cyclic dust accumulation during MIS 2 in Central Asia inferred from loess OSL dating and grain-size analysis. *Scientific Reports*, 6, e32365.
- Li, Y., Song, Y. G., Yan, L. B., Chen, T., & An, Z. S. (2015). Timing and spatial distribution of loess in Xinjiang, NW China. *PLoS One*, 10(5), e0125492.
- Liu, T. S. (1985). *Loess and the Environment*. (pp. 1–251). Beijing: China Ocean Press.
- Long, H., & Shen, J. (2014). Underestimated ^{14}C -based chronology of late Pleistocene high lake-level events over the Tibetan plateau and adjacent areas: Evidence from the Qaidam Basin and Tengger Desert. *Science China Earth Sciences*, 58(2), 183–194.
- Lu, Y. C., Wang, X. L., & Wintle, A. G. (2007). A new OSL chronology for dust accumulation in the last 130,000 yr for the Chinese Loess Plateau. *Quaternary Research*, 67(1), 152–160.
- Machalett, B., Frechen, M., Hambach, U., Oches, E. A., Zöller, L., & Marković, S. B. (2006). The loess sequence from Remisowka (northern boundary of the Tien Shan Mountains, Kazakhstan)—Part I: Luminescence dating. *Quaternary International*, 152–153, 192–201.
- Moine, O., Antoine, P., Hatte, C., Landais, A., Mathieu, J., Prud'homme, C., & Rousseau, D. D. (2017). The impact of last glacial climate variability in west-European loess revealed by radiocarbon dating of fossil earthworm granules. *Proceedings of the National Academy of Sciences*, 114(24), 6209–6214.
- Murray, A. S., & Wintle, A. G. (2000). Luminescence dating of quartz using an improved single-aliquot regenerative-dose protocol. *Radiation Measurements*, 32(1), 57–73.
- Murray, A. S., & Wintle, A. G. (2003). The single aliquot regenerative dose protocol: Potential for improvements in reliability. *Radiation Measurements*, 37(4), 377–381.
- Nian, X., Bailey, R. M., & Zhou, L. (2012). Investigations of the post-IR IRSL protocol applied to single K-feldspar grains from fluvial sediment samples. *Radiation Measurements*, 47(9), 703–709.
- Pigati, J. S., Mcgeehin, J. P., Muhs, D. R., & Bettis, E. A. (2013). Radiocarbon dating late Quaternary loess deposits using small terrestrial gastropod shells. *Quaternary Science Reviews*, 76, 114–128.
- Pigati, J. S., Mcgeehin, J. P., Muhs, D. R., Grimley, D. A., & Nekola, J. C. (2015). Radiocarbon dating loess deposits in the Mississippi Valley using terrestrial gastropod shells (Polygyridae, Helicinidae, and Discidae). *Aeolian Research*, 16, 25–33.
- Pigati, J. S., Quade, J., Wilson, J., Jull, A. J. T., & Lifton, N. A. (2007). Development of low-background vacuum extraction and graphitization systems for ^{14}C dating of old (40–60ka) samples. *Quaternary International*, 166(1), 4–14.
- Prescott, J. R., & Hutton, J. T. (1994). Cosmic ray contributions to dose rates for luminescence and ESR dating: Large depths and long-term time variations. *Radiation Measurements*, 23(2–3), 497–500.
- Prud'homme, C., Antoine, P., Moine, O., Turpin, E., Huguenard, L., Robert, V., & Degeai, J.-P. (2015). Earthworm calcite granules: A new tracker of millennial-timescale environmental changes in last glacial loess deposits. *Journal of Quaternary Science*, 30(6), 529–536.
- Qin, J., & Zhou, L. (2017). Luminescence dating of the Zeketai loess section in the Ili Basin, northwestern China: Methodological considerations. *Journal of Asian Earth Sciences*, in press, <https://doi.org/10.1016/j.jseaes.2017.1011.1018>
- Reimer, P. J., Reimer, R. W., & Blaauw, M. (2013). Radiocarbon dating | calibration of the ^{14}C record. *Encyclopedia of Quaternary Science*, 345–352.
- Roberts, H. M. (2008). The development and application of luminescence dating to loess deposits: A perspective on the past, present and future. *Boreas*, 37(4), 483–507.
- Shi, Z. T. (2005). The age of loess sediments in Yili area of Xinjiang and its paleoenvironment significances, Institute of Earth Environment, Chinese Academy of Sciences, Xi'an.
- Shi, Z., Dong, M., & Fang, X. (2007). The characteristics of late Pleistocene loess-paleosol magnetic susceptibility in Yili Basin. *Journal of Lanzhou University(Natural Sciences)*, 43(2), 7–10 (in Chinese with English abstract).
- Song, Y. G. (2012). Paleoclimatic implication of temperature-dependence of susceptibility of Tianshan loess, Central Asia. *Advanced Science Letters*, 6, 167–172.
- Song, Y. G., Chen, X. L., Qian, L. B., Li, C. X., Li, Y., Li, X. X., ... An, Z. S. (2014). Distribution and composition of loess sediments in the Ili Basin, Central Asia. *Quaternary International*, 334(12), 61–73.
- Song, Y. G., Lai, Z. P., Li, Y., Chen, T., & Wang, Y. X. (2015). Comparison between luminescence and radiocarbon dating of late Quaternary loess from the Ili Basin in Central Asia. *Quaternary Geochronology*, 30, 405–410.
- Song, Y. G., Li, C. X., Zhao, J. D., Chen, P., & Zeng, M. (2012). A combined luminescence and radiocarbon dating study of the Ili loess, Central Asia. *Quaternary Geochronology*, 10, 2–7.
- Song, Y. G., Li, Y., Li, Y., An, Z., Cheng, L., Sun, H., & Rustam, O. (2017). North Atlantic abrupt climate signals during the last glacial period in Central Asia: Evidences from aeolian loess sediments. *Acta Geologica Sinica-English Edition*, 91(4), 1135–1136.
- Song, Y. G., Nie, J. S., Shi, Z. T., Wang, X. L., Qiang, X. K., & Chang, H. (2010). A preliminary study of magnetic enhancement mechanisms of the Tianshan loess. *Journal of Earth Environment*, 1(1), 60–67.
- Song, Y. G., Shi, Z. T., Fang, X. M., Nie, J. S., Naoto, I., Qiang, X. K., & Wang, X. L. (2010). Loess magnetic properties in the Ili Basin and their correlation with the Chinese Loess Plateau. *Science China Earth Sciences*, 53(3), 419–431.
- Song, Y. G., Zeng, M. X., Chen, X. L., Li, Y., Chang, H., An, Z. S., & Guo, X. H. (2017). Abrupt climatic events recorded by the Ili loess during the last glaciation in Central Asia: Evidence from grain-size and minerals. *Journal of Asian Earth Sciences*, in press, <https://doi.org/10.1016/j.jseaes.2017.1010.1040>.
- Trauerstein, M., Lowick, S. E., Preusser, F., & Schlunegger, F. (2014). Small aliquot and single grain IRSL and post-IR IRSL dating of fluvial and alluvial sediments from the Pativilca valley, Peru. *Quaternary Geochronology*, 22(Supplement C), 163–174.
- Ujvari, G., Molnar, M., Novothny, A., & Kovacs, J. (2014). Lessons from the AMS ^{14}C and OSL/IRSL-dating of the Dunaszekcső loess record, Hungary. In *Loessfest'14 and 7th Loess Seminar*. Wroclaw, 26–27.
- Wang, Z., Zhao, H., Dong, G., Zhou, A., Liu, J., & Zhang, D. (2014). Reliability of radiocarbon dating on various fractions of loess-soil sequence for Dadiwan section in the western Chinese loess plateau. *Frontiers of Earth Science*, 8(4), 540–546.
- Yang, S. L., Forman, S. L., Song, Y. G., Pierson, J., Mazzocco, J., Li, X. X., ... Fang, X. M. (2014). Evaluating OSL-SAR protocols for dating quartz grains from the loess in Ili Basin, Central Asia. *Quaternary Geochronology*, 20, 78–88.
- Ye, W. (2001). *Sedimentary characteristics of loess and paleoclimate in westerly region of Xinjiang*. Beijing: China Ocean press.
- Ye, W., Dong, G., Yuan, Y., & Ma, Y. (2000). Climate instability in the Yili region, Xinjiang during the last glaciation. *Chinese Science Bulletin*, 45(17), 1603–1608.
- Youn, J. H., Seong, Y. B., Choi, J. H., Abdrakhmatov, K., & Ormukov, C. (2014). Loess deposits in the northern Kyrgyz Tien Shan: Implications for the paleoclimate reconstruction during the late Quaternary. *Catena*, 117, 81–93.
- Zech, M., Kreutzer, S., Zech, R., Goslar, T., Meszner, S., McIntyre, C., ... Fuchs, M. (2017). Comparative ^{14}C and OSL dating of loess-paleosol sequences to evaluate post-depositional contamination of n-alkane biomarkers. *Quaternary Research*, 87(1), 180–189.

- Zhang, W. X., Shi, Z. T., Chen, G. J., Liu, Y., Niu, J., Ming, Q. Z., & Su, H. (2013). Geochemical characteristics and environmental significance of Taledo loess-paleosol sequences of Ili Basin in Central Asia. *Environmental Earth Sciences*, 70(5), 2191–2202.
- Zhou, W., Cheng, P., Jull, A. J. T., Lu, X., An, Z., Wang, H., ... Wu, Z. (2016). ^{14}C Chronostratigraphy for Qinghai Lake in China. *Radiocarbon*, 56(01), 143–155.

How to cite this article: Song Y, Luo D, Du J, et al. Radiometric dating of late Quaternary loess in the northern piedmont of South Tianshan Mountains: Implications for reliable dating. *Geological Journal*. 2018;53(S2):417–426. <https://doi.org/10.1002/gj.3129>